Letter

Tuning the phonon transport in bilayer graphene to an anomalous regime dominated by electron-phonon scattering

Xiaolong Yang,[1,2] Zhe Liu,[1,3] Fanchen Meng,[4] and Wu Li[1,*]

[1]*Institute for Advanced Study, Shenzhen University, Shenzhen 518060, China*

[2]*College of Physics, and Center of Quantum Materials and Devices, Chongqing University, Chongqing 401331, China*

[3]*College of Physics and Optoelectronic Engineering, Shenzhen University, Shenzhen 518060, China*

[4]*Department of Physics and Astronomy, Clemson University, Clemson, South Carolina 29634, USA*

(Received 18 June 2021; revised 18 September 2021; accepted 21 September 2021; published 30 September 2021)

Recent studies have revealed the significance of electron-phonon interaction (EPI) in phonon transport at intermediate temperatures. In some metals, the EPI can even dominate over the anharmonic phonon-phonon (ph-ph) scattering, leading to an anomalous phonon transport regime in which the lattice thermal conductivity κ_L becomes nearly temperature (T) independent in contrast to the usual $1/T$ dependence. However, the experimental verification of this anomalous transport regime is very challenging due to the difficulty in separating the phonon contributions from the dominating electron ones to the measured total thermal conductivity in metals. In this work, using first-principles calculations, we predict that in bilayer graphene, the phonon transport can be driven to the anomalous regime by tuning the doping level. At high doping levels close to the Van Hove singularity, the EPI can result in a fivefold reduction of κ_L at room temperature, and κ_L becomes T independent. This anomalous behavior is found to have its origin in three aspects: (i) mirror symmetry breaking enables direct coupling between flexural phonons, the dominant carriers of κ_L, and electrons; (ii) dominance of normal processes in the anharmonic ph-ph scattering facilitates the EPI to be more prominent; (iii) dominance of these normal ph-ph processes induces the indirect effect of EPI on κ_L. This is distinct from monolayer graphene, where the mirror symmetry prohibits the direct scattering of the flexural phonons by electrons and only the indirect EPI affects κ_L. This work gives insight into the manipulation of heat conduction via externally induced EPI in two-dimensional materials in which mirror symmetry breaks and normal processes dominate the ph-ph scattering.

DOI: 10.1103/PhysRevB.104.L100306

The electron-phonon interaction is a fundamental quantity in condensed matter physics, essential for many physical properties including electrical transport, superconductivity, and optical absorption [1–3]. While the effect of the electron-phonon interaction (EPI) on electrical transport has been extensively studied, its impact on phonon transport, especially in nonmetals, was rarely explored, as the EPI was long believed to affect phonon transport only at very low temperatures. Only recently the EPI has been identified to have a significant role in lattice thermal conductivity in certain materials even at room temperature (RT). Liao *et al.* predicted [4] that, by adjusting the carrier concentration n, the EPI can result in up to 45% reduction of κ_L in heavily doped silicon even at RT, pioneering first principles investigation of the EPI effect on κ_L. This effect was subsequently observed experimentally [5]. It was also found that the phonon-electron (ph-e) scattering is much stronger than the phonon-phonon (ph-ph) scattering in a few transition metal carbides and the group-VI metals [6–9], giving rise to an anomalous phonon transport regime in which κ_L is nearly T independent. It is important to note that usually the electronic contribution dominates the thermal conductivity in metals and that it is difficult to separate the phononic and electronic contributions. These make the experimental verification of the anomalous regime very challenging. Furthermore, the EPI is an intrinsic and thus unadjustable scattering mechanism in metals. In contrast, the EPI in nonmetals, serving as an extrinsic scattering mechanism, can be largely tuned by changing carrier concentration. However, though EPI can play an important role, it has been found not strong enough to lead to the anomalous transport behavior in realistic systems so far, e.g., a reduction of less than 50% and a nonweak T dependence of thermal conductivity ($\kappa_L \propto T^{-\alpha}, \alpha > 0.6$) in p-type Si [4], n-type 3C-SiC [10], and p-type silicene [11]. In this context, whether the anomalous phonon transport regime can be achieved in a realistic system by manipulating the carrier concentration is of great importance not only from the fundamental point of view but also for practical applications.

Graphene, a representative of two-dimensional (2D) semimetals, has attracted much attention because of its record-high κ_L [12,13]. Despite intensive efforts to study phonon transport in MLG and the fact that high charge carrier densities of $|n| > 5.5 \times 10^{14}$ cm^{-2} can be achieved by fabricating electrolytic and ionic-liquid gates [14–18], the effect of EPI on its κ_L, however, had never been studied, as the EPI was thought to have little effect on its κ_L due to the fact that the flexural acoustic (ZA) phonons, the dominant carriers of κ_L, cannot interact with electrons directly due to the mirror symmetry [19]. Notably, our recent *ab initio* study [20] has

*wu.li.phys2011@gmail.com

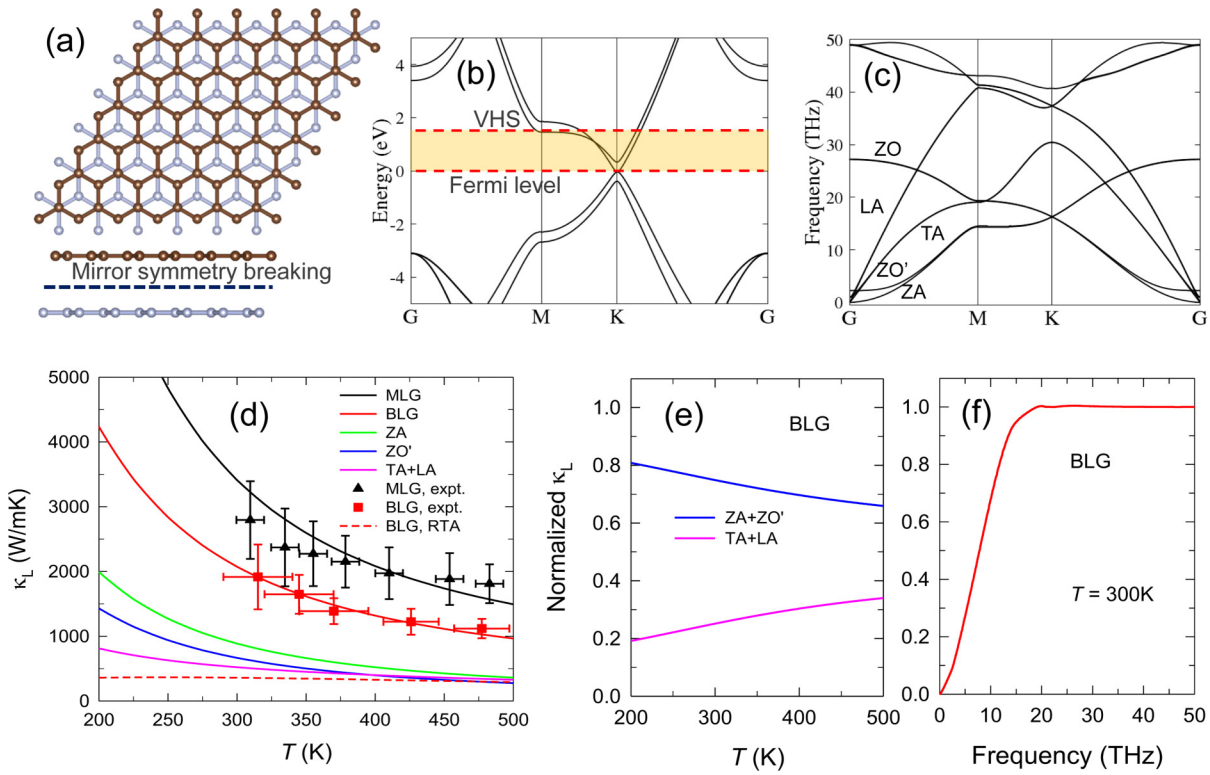

FIG. 1. (a) The side and top views of the lattice structure of *AB*-stacked BLG, with different colors labelling different layers. (b) The electronic structure of BLG, with the orange shading representing the range of Fermi levels tuned by the carrier density. (c) The phonon dispersion of BLG. ZA denotes the flexural acoustic phonons, and ZO′ and ZO represent the flexural optical phonons. TA and LA denote the transversal and longitudinal acoustic modes, respectively. (d) T-dependent κ_L for pristine MLG and BLG. (e) The relative contributions from the flexural phonons (ZA + ZO′) and other acoustic phonons (TA + LA). (f) The normalized cumulative κ_L at 300 K.

demonstrated that although the ZA phonons cannot be scattered by electrons directly, the indirect interaction between the ZA phonons and electrons enables 21% reduction of κ_L at RT in n-doped monolayer graphene (MLG). The excellent thermal transport behavior persists in bilayer graphene (BLG). Although the κ_L of BLG is significantly reduced compared with MLG due to the cross-plane coupling of phonons induced by the van der Waals (vdW) interactions between layers [21,22], recent studies [21,23–25] have shown that the κ_L of BLG is still as high as ∼2000 W/mK, comparable to diamond [26]. It is also important to note that, distinct from MLG, the flexural phonons in *AB*-stacked BLG can be directly scattered by electrons due to the mirror symmetry breaking with respect to the basal plane, as seen in Fig. 1(a). The EPI is thus expected to have stronger effect on κ_L in BLG than in MLG.

In this Letter, by performing density functional calculations, we predict that the EPI can lead to the anomalously weak T dependence and a large reduction (up to fivefold) of κ_L at high doping levels in *AB*-stacked BLG, enabling the experimental verification of the EPI-induced anomalous phonon transport regime. Such an ultrastrong effect is found to originate from the direct coupling between the flexural phonons and electrons induced by the mirror symmetry breaking, together with the dominance of normal ph-ph scattering.

Here the thermal conductivity is calculated by exactly solving the phonon Boltzmann transport equation (BTE) using an iterative scheme starting with the relaxation time approximation (RTA), and phonon lifetimes due to the isotope, anharmonic three-phonon, and ph-e scatterings are included. See more details in Sec. 1 of the Supplemental Material [27] (see, also, Refs. [9,28–34] therein).

Solving the BTE requires electron energies, phonon frequencies, and anharmonic interatomic force constants, which were calculated from density-functional theory and density-functional perturbation theory, as implemented in the QUANTUM-ESPRESSO package [35]. The EPW package [36] was employed to calculate the ph-e scattering rates. The SHENGBTE package [28,37,38] was modified to incorporate the ph-e scattering rates and then used to solve the BTE. Full computational details are shown in Sec. 2 of the Supplemental Material [27] (see, also, Refs. [39–42] therein).

We first study the intrinsic thermal transport properties of BLG. Our calculated phonon dispersion of BLG is presented in Fig. 1(d). It clearly shows that the interlayer vdW interaction causes the the original ZA mode to split into the ZA and ZO′ modes, with the latter being a so-called layer breathing mode [43,44] and corresponding to the out-of-plane relative motion of atoms. Due to the splitting, the ZA branch of BLG in the long-wave limit ($\mathbf{q} \to \mathbf{0}$) is no longer strictly quadratic [45]. As a consequence, the four-phonon scattering in BLG should be unimportant as demonstrated in Ref. [46], and hence in the present work we consider phonon anharmonicity only up to the third order. Also, the existence of the breathing mode could bring in more three-phonon scattering channels

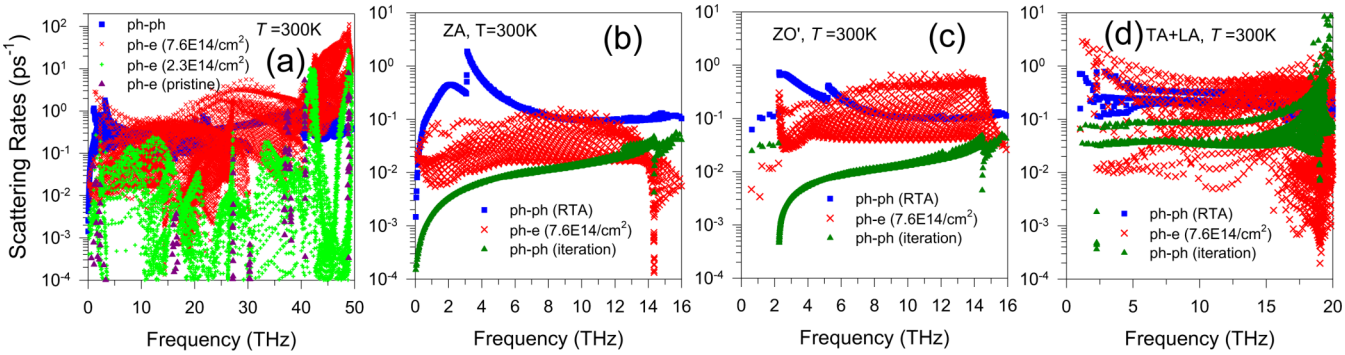

FIG. 2. (a) Comparison of the intrinsic ph-ph and ph-e scattering rates at different carrier densities in BLG at 300 K, calculated within the RTA. Comparison of ph-ph and ph-e scattering rates of (b) ZA, (c) ZO′, and (d) TA and LA modes for phonons below 20 THz in doped BLG with $n = 7.6 \times 10^{14}$ cm^{-2}. Both the ph-ph scattering rates determined by the RTA and by the exact solution are provided.

involving ZA phonons, implying the stonger three-phonon scattering of ZA modes for BLG than for MLG.

Figure 1(d) shows the T-dependent κ_L for pristine MLG and BLG. Our calculations show reasonable agreement with the measured data [47]. It can be seen that with one layer added, the κ_L at RT decreases from ∼3412 to 2073 W/mK, by over 29%. Also shown is the κ_L calculated within the RTA for BLG, which is significantly lower than the exact values from the iterative solution over the entire T range. The severe underestimation of κ_L by the RTA signifies the dominance of momentum-conserved normal processes over umklapp processes in the ph-ph scattering of BLG. By further decomposing κ_L into different branches, we can see that below 400 K the κ_L is always dominated by the ZA and ZO′ branches. To examine this more fully, in Fig. 1(f) we show the relative contributions to κ_L from the ZA and ZO′ modes ($\kappa_L^{\mathrm{ZA+ZO'}}$) and other acoustic modes ($\kappa_L^{\mathrm{TA+LA}}$). It is evident that $\kappa_L^{\mathrm{ZA+ZO'}}$ gives the dominant contribution over the entire T range. At RT, $\kappa_L^{\mathrm{ZA+ZO'}}$ provides 75% of the total κ_L, and $\kappa_L^{\mathrm{TA+LA}}$ gives ∼25%. Figure 1(g) also displays the cumulative κ_L of BLG, which indicates that the κ_L is determined by phonons with frequency below 20 THz.

In the pristine case, the effect of EPI on the κ_L of BLG is negligible, as only some phonons around $\mathbf{\Gamma}$ and $\mathbf{K}$ characterized by certain discrete frequencies can be scattered by electrons, similarly as in MLG [20]. As is seen in Fig. 2(a), in the neutral BLG, the ph-e scattering rates are considerably lower than the intrinsic ph-ph scattering rates. Recent studies have shown that high doping levels close to or even beyond the Van Hove singularity (VHS) [corresponding to the upper bound of the shading region in Fig. 1(c)] can be achieved [14–18]. In the doping case, more electrons are able to efficiently participate in the ph-e scattering processes, and consequently the region in the Brillouin zone (BZ) where phonons can be scattered broadens around $\mathbf{\Gamma}$ and $\mathbf{K}$. From Fig. 2(a), it is clear that the ph-e scattering rates significantly increase with n, and phonons in the whole BZ can be scattered by electrons above $n = 2.3 \times 10^{14}$ cm^{-2}. For the case of $n = 7.6 \times 10^{14}$ cm^{-2} (corresponding to the VHS) in particular, the ph-e scattering rates for phonons with frequency below 20 THz, which have a major contribution to κ_L, are comparable to or even higher than the ph-ph scattering rates.

Since the κ_L of BLG is determined by the ZA, ZO′, as well as TA and LA phonons, we further compare the scattering rates due to ph-e and ph-ph scatterings for these modes. The results are given in Figs. 2(b)–2(d). Unlike MLG, the flexural phonons in BLG can be directly scattered by electrons owing to the mirror symmetry breaking. As is seen in Figs. 2(b) and 2(c), when n reaches 7.6×10^{14} cm^{-2}, the ph-e scattering rates of ZA and ZO′ modes are comparable to or even surpass their ph-ph scattering rates. As for the TA and LA modes, the scattering rates of phonons with frequency below 20 THz are dominated by ph-e scattering, as seen in Fig. 2(d).

As mentioned above, the large discrepancy between the RTA and iteration reveals the dominance of normal ph-ph scattering in BLG. Hence, the intrinsic ph-ph scattering given by the RTA is significantly stronger than that given by the iterative solution to the BTE. As is seen in Figs. 2(b)–2(d), the ph-e scattering rates of ZA and ZO′ as well as TA and LA modes are substantially larger than the ph-ph scattering rates from the iterative solution. This indicates that the EPI may dominate the thermal transport of BLG at high doping levels.

The calculated T-dependent κ_Ls of BLG for several carrier densities as well as the pristine case are shown in Fig. 3(a). It clearly shows that the EPI can tune the phonon transport of BLG to an anomalous regime. Interestingly, at high carrier densities, e.g., $n = 7.6 \times 10^{14}$ cm^{-2}, the κ_L is found to be almost independent of T (exactly $\kappa_L \sim T^{-0.078}$), deviating from the T^{-1} law governed by three-phonon scattering. The ph-e scattering is nearly T independent because of the almost T-independent term of $f_{\mathbf{k}i} - f_{(\mathbf{k}+\mathbf{q})j}$ in the formula of EPI [see Eq. (S5) in the Supplemental Material [27]], with $f_{\mathbf{k}i}$ being the Fermi-Dirac distribution function with band branch i and wave vector $\mathbf{k}$. Therefore, this anomalous weak T dependence of κ_L is due to the predominance of the nearly T-independent ph-e over the T-dependent ph-ph scattering, which has been reported in some metals [6,7] but not in nonmetals yet. To look into the carrier dependence more closely, the RT κ_L varying with a series of carrier densities are given in Fig. 3(b). It is found that when n is below 7.8×10^{13} cm^{-2}, the EPI effect on κ_L is negligible, whereas the EPI leads to significant reduction of lattice thermal conductivity as n reaches above 1.4×10^{14} cm^{-2}. Remarkably, when n is as high as 7.6×10^{14} cm^{-2}, the EPI decreases the κ_L from ∼2073 W/mK in the pristine case to ∼400 W/mK at RT, by 80%. This exceptionally strong EPI effect on κ_L has

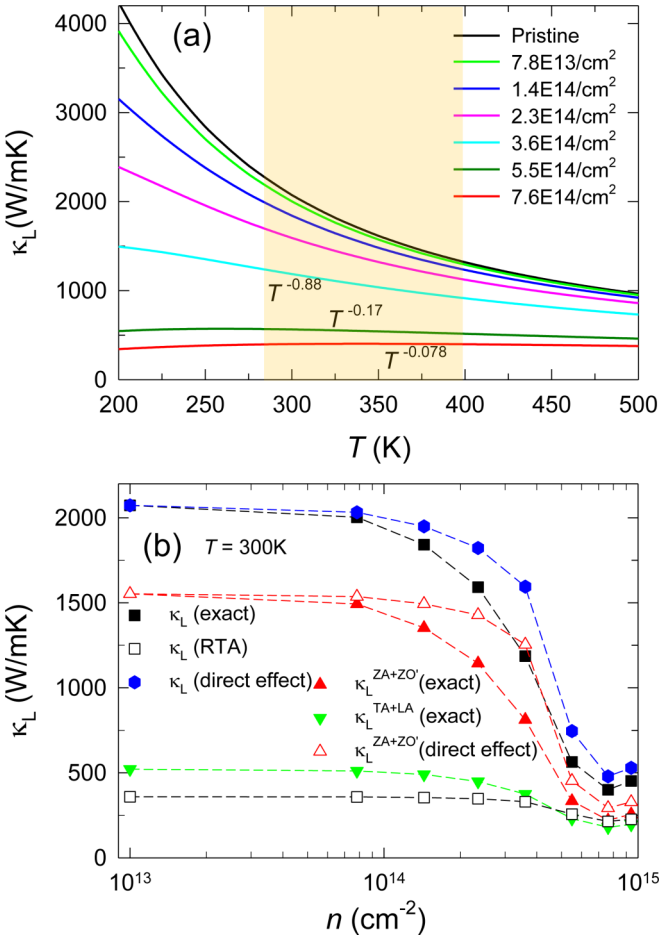

FIG. 3. (a) The calculated T-dependent κ_L of BLG at different carrier densities. (b) The values of κ_L, $\kappa_L^{ZA+ZO'}$, and κ_L^{TA+LA} determined from the exact BTE solution, and κ_L from the RTA as a function of n at RT. To highlight the direct EPI effect, the κ_L and $\kappa_L^{ZA+ZO'}$ calculated within the BTE in which ph-e processes are not included in the iteration are also shown.

its origin in direct interaction between flexural phonons and electrons, weak ph-ph scattering enabled by strong normal scatterings, and indirect coupling between flexural phonons and electrons, which will be elaborated in detail in the following.

First, we look into the EPI effect on thermal conductivity at the RTA level in Fig. 3(b). In the case of $n = 7.6 \times 10^{14}$ cm^{-2}, within the RTA the EPI reduces κ_L by 41% at RT, much lower than the actual reduction given by the iterative solution. As the dominant contributors of κ_L, the flexural phonons' contributions are obviously suppressed by the direct coupling between flexural phonons and electrons enabled by the mirror symmetry breaking, e.g., κ_L^{ZA} is decreased from 68 to 51 W/mK at RT, by 25%, as seen in Table I. This is completely different from MLG, where κ_L^{ZA} cannot be affected by the EPI due to the mirror symmetry [20]. In fact, the RTA improperly treats the normal ph-ph scatterings as fully resistive processes, thus it overestimates the intrinsic ph-ph scattering and consequently underestimates the EPI effect on κ_L. To quantify the EPI effect more accurately, a natural way is to calculate the total phonon lifetime by directly summing up

TABLE I. The calculated κ_L and contributions from different branches for the pristine and doped ($n = 7.6 \times 10^{14}$ cm^{-2}) BLG at RT, predicted from the RTA and the iterative solution, respectively.

	Pristine		$n = 7.6 \times 10^{14}$ cm^{-2}	
κ_L (W/mK)	RTA	Iteration	RTA	Iteration
ZA	68	887	51	139
ZO′	61	666	30	82
TA+LA	213	518	125	175
Total	360	2073	214	400

the ph-ph scattering rates given by the iterative solution and ph-e scattering rates, with the details given in Sec. 1 of the Supplemental Material [27]. We then apply this approximation to evaluate the EPI effect, as shown in Fig. 3(b), and find that the EPI can reduce the κ_L by 77%, still lower than the actual reduction. The underestimation of 3% is due to the fact that this approach cannot incorporate the indirect EPI effect, which is important when normal processes dominate. Actually, in MLG there exists only indirect effect between the ZA phonons and electrons mediated by the TA and LA phonons, leading to 21% reduction of κ_L [20]. Note that this approximation has been utilized recently [48,49].

To simultaneously include the indirect effect of EPI, only an iterative solution is appropriate. Note that since each ph-e scattering process involves one phonon only, the iterative form of the BTE after including EPI is the same as it is without including EPI (see Sec. 1 of the Supplemental Material [27]). With the indirect EPI effect included through the iterative scheme, we show that the EPI leads to 80% reduction of κ_L. As seen in Fig. 3(b), the indirect EPI effect is reflected in the difference of thermal conductivity (κ_L and $\kappa_L^{ZA+ZO'}$) obtained from these two approaches. Specifically, the direct EPI effect alone reduces the $\kappa_L^{ZA+ZO'}$ by 81% and after including the indirect effect the $\kappa_L^{ZA+ZO'}$ is reduced by 85%. Also, we can see from Table I that the reduction of contributions from different branches due to the EPI after the iteration is several times larger than before the iteration. This indicates that the dominance of normal ph-ph scatterings plays a key role in achieving such an ultrastrong EPI effect on κ_L by magnifying the direct EPI effect and introducing the indirect EPI effect.

The present results emphasize the significance of externally induced EPI in suppressing the κ_L of BLG. We have to point out that such an ultrastrong effect is not limited to graphene but should be universal in many other 2D materials such as h-BX (X = N, P, and As) and h-AlN [50,51], for which (i) flexural phonons give a major contribution to κ_L; (ii) normal processes dominates the ph-ph scattering. This is quite different from materials like silicon [4] and silicene [11], for which even at high carrier density limit the EPI decreases κ_L by less than 50%, as the dominance of umklapp processes makes the ph-ph scattering always stronger than the ph-e scattering. Note also that in the present work the κ_L is calculated within the decoupled BTE, where electrons are taken to be in equilibrium when solving the BTE, and the electron drag effect is thus not included. As mentioned previously [52,53], the electron drag effect on the thermal conductivity is generally weak, since the drag effect only

affects the low-energy and zone-boundary phonons, which give the little contribution to κ_L. For MLG, it has been proven that umklapp processes dominate the e-ph scattering (electron scattering by phonons), which can bring quickly the electrons into equilibrium with the lattice, and the electron drag effect is thus negligible [20]. The same case also applies to BLG (see Sec. 4 of the Supplemental Material [27] and Refs. [54,55] therein).

To summarize, we have identified a marked EPI effect on the lattice thermal conductivity of BLG by first-principles calculations. Our results show that the EPI can result in the fundamentally different T dependencies of κ_L, and it can reduce the κ_L of BLG by as much as a factor of 5 even at RT. This is enabled by the combined effect of direct coupling between the flexural phonons and electrons induced by the mirror symmetry breaking, as well as the dominance of normal ph-ph scattering. This EPI-driven anomalous phonon transport regime in BLG calls for the future experimental verification, and can be extended to other 2D materials.

W.L. acknowledges support from the GuangDong Basic and Applied Basic Research Foundation (Grant No. 2021A1515010042), the Stable Support Plan of the Higher Education Institutions of Shenzhen (Grant No. 20200809161605001), the Shenzhen Science, Technology and Innovation Commission (Grant No. JCYJ20170412105922384) and the Natural Science Foundation of China (NSFC) (Grant No. 11704258). X.Y. acknowledges support from the NSFC (Grant No. 12004254) and the startup funding granted by Chongqing University (Grant No. 0233001104472).

[1] J. M. Ziman, *Electrons and Phonons: The Theory of Transport Phenomena in Solids*, International series of monographs on physics (Clarendon, Oxford, 1960).
[2] P. Y. Yu, M. Cardona, P. Y. Yu, and M. Cardona, in *Fundamentals of Semiconductors: Physics and Materials Properties* (Springer, Berlin, 2010), pp. 1–15.
[3] F. Giustino, Rev. Mod. Phys. **89**, 015003 (2017).
[4] B. Liao, B. Qiu, J. Zhou, S. Huberman, K. Esfarjani, and G. Chen, Phys. Rev. Lett. **114**, 115901 (2015).
[5] J. Zhou, H. D. Shin, K. Chen, B. Song, R. A. Duncan, Q. Xu, A. A. Maznev, K. A. Nelson, and G. Chen, Nat. Commun. **11**, 6040 (2020).
[6] C. Li, N. K. Ravichandran, L. Lindsay, and D. Broido, Phys. Rev. Lett. **121**, 175901 (2018).
[7] Y. Chen, J. Ma, and W. Li, Phys. Rev. B **99**, 020305(R) (2019).
[8] A. Kundu, J. Ma, J. Carrete, G. Madsen, and W. Li, Mater. Today Phys. **13**, 100214 (2020).
[9] S. Wen, J. Ma, A. Kundu, and W. Li, Phys. Rev. B **102**, 064303 (2020).
[10] T. Wang, Z. Gui, A. Janotti, C. Ni, and P. Karandikar, Phy. Rev. Mater. **1**, 034601 (2017).
[11] S.-Y. Yue, R. Yang, and B. Liao, Phys. Rev. B **100**, 115408 (2019).
[12] A. A. Balandin, S. Ghosh, W. Bao, I. Calizo, D. Teweldebrhan, F. Miao, and C. N. Lau, Nano Lett. **8**, 902 (2008).
[13] J. H. Seol, I. Jo, A. L. Moore, L. Lindsay, Z. H. Aitken, M. T. Pettes, X. Li, Z. Yao, R. Huang, D. Broido *et al.*, Science **328**, 213 (2010).
[14] D. K. Efetov and P. Kim, Phys. Rev. Lett. **105**, 256805 (2010).
[15] J. L. McChesney, A. Bostwick, T. Ohta, T. Seyller, K. Horn, J. Gonzalez, and E. Rotenberg, Phys. Rev. Lett. **104**, 136803 (2010).
[16] J. Ye, M. F. Craciun, M. Koshino, S. Russo, S. Inoue, H. Yuan, H. Shimotani, A. F. Morpurgo, and Y. Iwasa, Proc. Natl. Acad. Sci. USA **108**, 13002 (2011).
[17] D. K. Efetov, P. Maher, S. Glinskis, and P. Kim, Phys. Rev. B **84**, 161412(R) (2011).
[18] P. Rosenzweig, H. Karakachian, D. Marchenko, K. Kuster, and U. Starke, Phys. Rev. Lett. **125**, 176403 (2020).
[19] M. V. Fischetti and W. G. Vandenberghe, Phys. Rev. B **93**, 155413 (2016).
[20] X. Yang, A. Jena, F. Meng, S. Wen, J. Ma, X. Li, and W. Li, Mater. Today Phys. **18**, 100315 (2021).
[21] S. Ghosh, W. Bao, D. L. Nika, S. Subrina, E. P. Pokatilov, C. N. Lau, and A. A. Balandin, Nat. Mater. **9**, 555 (2010).
[22] Z. Wei, Z. Ni, K. Bi, M. Chen, and Y. Chen, Carbon **49**, 2653 (2011).
[23] Z. Wang, R. Xie, C. T. Bui, D. Liu, X. Ni, B. Li, and J. T. L. Thong, Nano Lett. **11**, 113 (2011).
[24] K. M. F. Shahil and A. A. Balandin, Nano Lett. **12**, 861 (2012).
[25] J. Wang, L. Zhu, J. Chen, B. Li, and J. T. L. Thong, Adv. Mater. **25**, 6884 (2013).
[26] J. R. Olson, R. O. Pohl, J. W. Vandersande, A. Zoltan, T. R. Anthony, and W. F. Banholzer, Phys. Rev. B **47**, 14850 (1993).
[27] See Supplemental Material at http://link.aps.org/supplemental/10.1103/PhysRevB.104.L100306 for methodology, computational details, convergence test of ph-e scattering rates and κ_L with respect to the q grids, and dominance of umklapp processes in the e-ph scattering.
[28] W. Li, J. Carrete, N. A. Katcho, and N. Mingo, Comput. Phys. Commun. **185**, 1747 (2014).
[29] D. A. Broido, M. Malorny, G. Birner, N. Mingo, and D. A. Stewart, Appl. Phys. Lett. **91**, 231922 (2007).
[30] A. Kundu, N. Mingo, D. A. Broido, and D. A. Stewart, Phys. Rev. B **84**, 125426 (2011).
[31] S.-i. Tamura, Phys. Rev. B **27**, 858 (1983).
[32] N. Bonini, M. Lazzeri, N. Marzari, and F. Mauri, Phys. Rev. Lett. **99**, 176802 (2007).
[33] W. Li, Phys. Rev. B **92**, 075405 (2015).
[34] A. Jain and A. J. H. McGaughey, Phys. Rev. B **93**, 081206(R) (2016).
[35] P. Giannozzi, S. Baroni, N. Bonini, M. Calandra, R. Car, C. Cavazzoni, D. Ceresoli, G. L Chiarotti, M. Cococcioni, I. Dabo, A. D. Corso, S. de Gironcoli, S. Fabris, G. Fratesi, R. Gebauer, U. Gerstmann, C. Gougoussis, A. Kokalj, M. Lazzeri, L. Martin-Samos, N. Marzari, F. Mauri, R. Mazzarello, S. Paolini, A. Pasquarello, L. Paulatto, C. Sbraccia, S. Scandolo, G. Sclauzero, A. P Seitsonen, A. Smogunov, P. Umari, and R. M Wentzcovitch, J. Phys.: Condens. Matter **21**, 395502 (2009).

[36] S. Poncé, E. R. Margine, C. Verdi, and F. Giustino, Comput. Phys. Commun. **209**, 116 (2016).
[37] W. Li, N. Mingo, L. Lindsay, D. A. Broido, D. A. Stewart, and N. A. Katcho, Phys. Rev. B **85**, 195436 (2012).
[38] W. Li, L. Lindsay, D. A. Broido, D. A. Stewart, N. Mingo, Phys. Rev. B **86**, 174307 (2012).
[39] N. Troullier and J. L. Martins, Phys. Rev. B **43**, 1993 (1991).
[40] J. Ihm, A. Zunger, and M. L. Cohen, J. Phys. C: Solid State Phys. **12**, 4409 (1979).
[41] S. Grimme, J. Comput. Chem. **27**, 1787 (2006).
[42] V. Barone, M. Casarin, D. Forrer, M. Pavone, M. Sambi, and A. Vittadini, J. Comput. Chem. **30**, 934 (2009).
[43] K. H. Michel and B. Verberck, Phys. Rev. B **78**, 085424 (2008).
[44] J.-A. Yan, W. Y. Ruan, and M. Y. Chou, Phy. Rev. B **77**, 125401 (2008).
[45] Y. Kuang, L. Lindsay, and B. Huang, Nano Lett. **15**, 6121 (2015).
[46] T. Feng and X. Ruan, Phys. Rev. B **97**, 045202 (2018).
[47] H. Li, H. Ying, X. Chen, D. L. Nika, A. I. Cocemasov, W. Cai, A. A. Balandin, and S. Chen, Nanoscale **6**, 13402 (2014).
[48] Y. Huang, J. Zhou, G. Wang, and Z. Sun, J. Am. Chem. Soc. **141**, 8503 (2019).
[49] C. Liu, M. Yao, J. Yang, J. Xi, and X. Ke, Mater. Today Phys. **15**, 100277 (2020).
[50] H. Fan, H. Wu, L. Lindsay, and Y. Hu, Phys. Rev. B **100**, 085420 (2019).
[51] H. Wang, L. Yu, J. Xu, D. Wei, G. Qin, Y. Yao, and M. Hu, Int. J. Therm. Sci. **162**, 106772 (2021).
[52] N. H. Protik and D. A. Broido, Phys. Rev. B **101**, 075202 (2020).
[53] N. H. Protik and B. Kozinsky, Phys. Rev. B **102**, 245202 (2020).
[54] R. C. Albers, L. Bohlin, M. Roy, and J. W. Wilkins, Phys. Rev. B **13**, 768 (1976).
[55] J. Zhou, B. Liao, and G. Chen, Semicond. Sci. Technol. **31**, 043001 (2016).